Intense-field Multiple-Detachment of F_2^-: Competition with Photodissociation

Abhishek Shahi†, *Yishai Albeck*†, *Daniel Strasser**

Institute of Chemistry, The Hebrew University of Jerusalem, 91904 Jerusalem, Israel.

ABSTRACT

The competition of intense-field multiple-detachment with efficient photodissociation of F_2^- is studied as a function of laser peak intensity. The main product channels are disentangled and characterized by 3D coincidence fragment imaging. The presented kinetic energy release spectra, angular distributions as well as two color pump-probe measurements allow identification of competing sequential and non-sequential mechanisms. Dissociative detachment, producing two neutral atoms (F + F) is found to be dominated by a sequential mechanism of photodissociation (F^- + F) followed by detachment of the atomic anion fragment. In contrast, dissociative ionization (F + F^+) shows competing contributions of both a sequential two-step mechanism as well as a non-sequential double-detachment of the molecular anion, which are distinguished by the kinetic energy released in the dissociation. Triple-detachment is found to be non-sequential in nature and results in Coulomb explosion (F^++F^+). Furthermore, the measured kinetic energy release for dissociation on the $^2\Sigma_g^+$ state provides a direct measurement of the F_2^- dissociation energy, D_0 = 1.26±0.03 eV.

KEYWORDS: Coincidence imaging, Intense-field, fs laser, Double detachment, Kinetic Energy Release, Rydberg states, Photodissociation, Photoionization, F_2^-, Dissociation energy

† Equal contributions

* Corresponding author, email: strasser@huji.ac.il

INTRODUCTION:

Intense laser pulse interactions with atomic and molecular anions are intrinsically different from interactions with overall neutral or positively charged systems.[1–5] For neutral systems, intuitive mechanisms such as tunnel ionization and rescattering can often provide a qualitative, as well as quantitative, description for intense-field processes including above threshold ionization, double ionization and high order harmonic generation (HHG).[6–13] In contrast, far less is known about intense-field interactions with anionic systems. Non-sequential as well as rescattering processes were considered to explain the experimentally measured high-energy photoelectron spectra emerging from intense-field interaction with atomic anions.[14–17] While sequential double-detachment was proposed by Bergues and Kiyan to account for measured photoelectron spectra with 100 fs pulses,[18] experiments with shorter laser pulses were shown to exhibit dominant non-sequential mechanisms.[2,5] Tentative initial assignment of a rescattering mechanism to the non-sequential double-detachment of atomic F^- was proposed by Pedregosa-Gutierrez *et al*.[2] Double-detachment of several molecular and cluster anion systems was found to be enhanced compared to atomic F^- system.[19] Nevertheless, studies as a function of polarization ellipticity for the atomic F^- as well as for several molecular and cluster anions were found to be not consistent with semiclassical rescattering dynamics.[5,19–21] Furthermore, Kandhasamy *et al.* proposed dissociation on highly excited $(SF_6^+)^*$ states with a dication core and a Rydberg electron to account for the observed $SF_5^+ + F$ events with high kinetic energy release (KER), produced by intense-field interaction with the molecular SF_6^- anion.[20] In the absence of a successful theoretical picture for intense-field interactions with anionic systems, it is important to experimentally examine the nature of intense-field multiple detachment of molecular anions.

In particular, it is appealing to explore the competition of photodissociation with multiple-detachment. Diatomic halogen anions exhibit low lying dissociative states that are accessible in the near-IR and can directly compete with the non-linear photodetachment process.[22–25] The 3.08 eV detachment energy and even higher vertical detachment of F_2^- make it a natural candidate for intense-field studies.[24–26] Indeed, Kiyan and co-workers interpreted F_2^- photoelectron spectrum measurements with intense 130 fs laser pulses as a combination of direct photodetachment and a sequential mechanism of photodissociation followed by photodetachment of the atomic product.[27] Interestingly, as opposed to diatomic halogen anions such as I_2^-, for which photodissociation was extensively studied,[23,28–30] less experimental data are available for the F_2^- photodissociation. Consequently, the dissociative $^2\Pi_g$, $^2\Pi_u$, and $^2\Sigma_g^+$ states of F_2^- were explored mainly through their role as resonances in dissociative attachment process.[24,31–35] Figure 1a shows the relevant potential curves of the F_2^- and F_2 systems.[31] Considering the ~1.55eV photon energy at the 800 nm wavelength, one can expect a

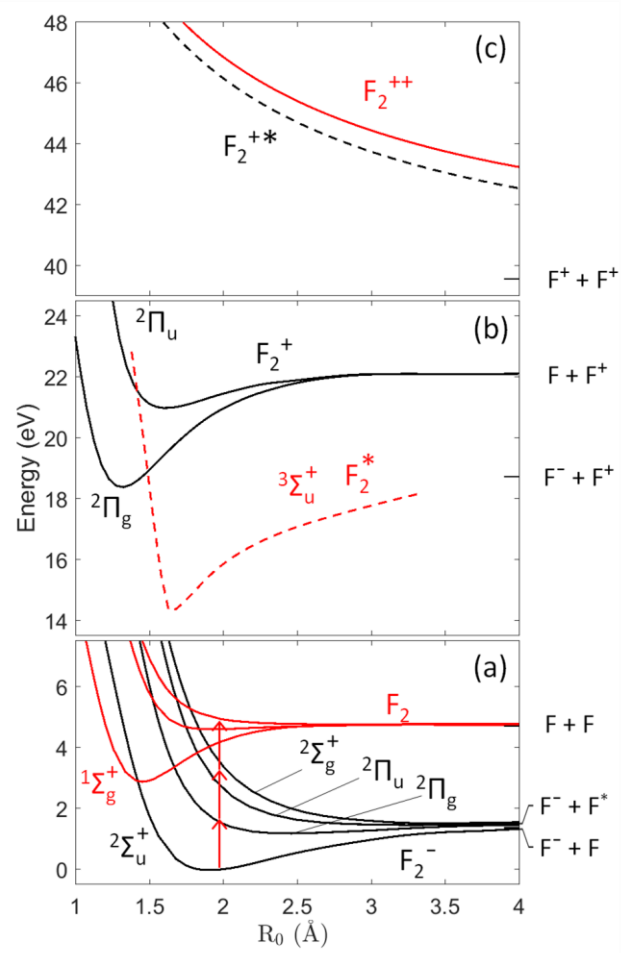

Figure 1: Potential energy curves of relevant F_2 systems. (a) The dark lines show the F_2^- $^2\Sigma_u^+$ ground state and relevant $^2\Pi_g$, $^2\Pi_u$ and $^2\Sigma_g^+$ dissociative states. Grey lines (red color online) show neutral F_2 states converging to the F + F limit.[31] (b) The full dark lines indicate the cationic F_2^+ potentials, while the dashed line (red online) indicates the estimated ion-pair curve leading to correlated F^+ and F^- products.[36] (c) The full line (red online) represents a Coulomb repulsion potential converging to the $F^+ + F^+$ limit, located ~39.5 eV above the anion ground state.[36] The dashed dark curve represents a high lying F_2^{+*} Rydberg state that in the short range mimics the Columbic repulsion of dicationic F_2^{++} core to an asymptotic $F^+ + F^*$ limit.

perpendicular photodissociation transition from the $^2\Sigma_u^+$ ground state to the $^2\Pi_g$ first excited state of F_2^-. One photon transition to the $^2\Pi_u$ state is forbidden by symmetry, but could be excited by a two-photon process. In comparison, vertical detachment of the F_2^- ground state would require absorption of 3 photons, which provide sufficient energy to dissociate the neutral product. The potential curves for the F_2^+ cation states are represented by the full lines in figure 1b, showing that ionization by removal of an additional electron would require a total of ~18eV,[36] corresponding to ~12 photons at 800 nm. Finally, the full line in figure 1c shows a Coulomb repulsion curve that dissociates into two correlated atomic cations ($F^+ + F^+$), indicating that removal of a third electron from the F_2^- system requires over ~45 eV.

In this paper we use 3D coincidence imaging of the correlated atomic fragments from a single F_2^- molecule at a time, to disentangle the competing dissociation, detachment and ionization processes. KER spectra and angular fragment distributions as well as time resolved 2-color pump-probe measurements are presented, describing the competing sequential and non-sequential mechanisms of intense laser pulse interaction with the molecular F_2^- anion.

EXPERIMENTAL SETUP:

The experimental apparatus was previously described in detail.[5,19–21,37] Briefly, cold anions are produced by a 200 eV pulsed electron gun in a supersonic expansion of argon carrier gas, seeded with ~2% NF_3 precursor gas sample at a total pressure of ~14 atm. Atomic F^- and molecular F_2^- species are produced by dissociative electron attachment to the NF_3 precursor.[38,39] After the expansion, the cold ions are accelerated up to E_0 ~2.36 keV kinetic energy in a pulsed Wiley−McLaren time-of-flight mass-spectrometer[40] that allows selecting ions with specific charge over mass ratio at the entrance to the photofragment spectrometer shown schematically in

Figure 2. Figure 2 inset shows a typical time of flight (TOF) spectrum, demonstrating the capability to separate the targeted F_2^- at 38 amu from lighter $F^-{\cdot}H_2O$ ions at 37 amu that arrive ~200 ns earlier to the photofragment spectrometer. Ions that are allowed to pass the mass gate deflector at the entrance of the spectrometer are further accelerated by the spectrometer potential (U_{SP} ~0.6 kV) before arriving to the field-free laser−ion interaction region. In the interaction region the ion beam is intersected by the optical path of a focused intense laser.[41] Two color ~35 fs pulses are implemented for the experiments presented here: an intense (~5 mJ) 800 nm pulse and a weaker (~100 μJ) 400 nm pulse prepared by doubling in a BBO crystal. The two colors are collinearly combined with a dichroic mirror at a computer controlled relative time delay. The dependence of different processes on the laser peak intensity is examined using only the intense 800 nm pulse and systematic displacement of a 250 mm focal length lens,[37] reaching up to ~10^{16} W/cm^2 at the focal spot. The response of the F_2^- anion to the increasing peak intensity is directly compared to the previously studied atomic F^- species,[19] by continuously alternating between the two species that are formed in the ion source, while maintaining the same laser conditions.

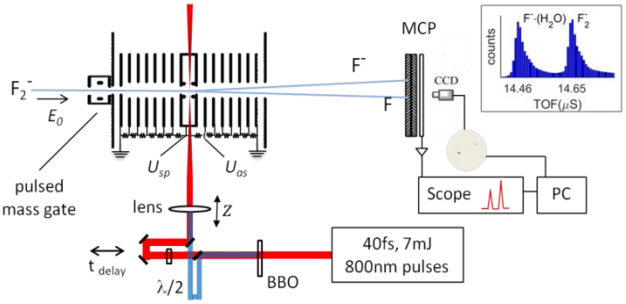

Figure 2: Schematic representation of experimental setup. Mass selected F_2^- ions interact with a focused intense fs laser pulse at the photofragment spectrometer ion-laser interaction region. The fragments are mass resolved by the U_{sp} photofragment spectrometer potential and detected in coincidence on a time and position sensitive detector located downstream of the photofragment spectrometer. Inset shows TOF spectrum resolving F_2^- and the adjacent $F^-{\bullet}H_2O$.

As photofragmentation events occur in the moving frame of the anion beam, all fragments continue towards the time and position sensitive micro-channel plate (MCP) detector located downstream of the photofragment spectrometer. The initial velocity of the parent anion molecule, corresponding to an E_0+U_{sp} kinetic energy, provides sufficient energy for detection of

all the charged as well as neutral photofragments that are separated according to their charge over mass ratios by the spectrometer potential, U_{sp}. Cationic products are accelerated, reaching the detector first, followed by neutral products of laser-ion interaction. Anion products are decelerated, thus separating the parent anions form negatively charged fragments that arrive last to the detector. In this way, all possible products including anionic F^-, neutral F and cationic F^+ species can be detected in coincidence.

For each laser pulse, the time and position of the correlated fragment hits on the MCP detector surface are acquired. The electronic timing signal from the MCP detector is digitized using a fast scope, while the 2D position information is read out optically from the P46 phosphor anode by a high frame rate CCD camera.[20] Both CCD exposure and scope acquisition times are synchronized to the laser pulse to record all the anionic, cationic and neutral products. Fast peak-finding routines are implemented to extract the TOFs and pulse amplitudes from the electronic signal as well as the 2D positions and brightness of the coincident optical signals. The optical and electronic signals are correlated based on their respective peak brightness and amplitude.[20,42,43] Thus, 3D velocities of the detected fragments are calculated in the molecular frame of reference, taking into account for each fragment the charge over mass, TOF and spectrometer potentials as obtained from detailed SIMION simulations of the experimental setup.[20,44] Furthermore, only true coincidence events are selected based on the calculated center of mass momentum of the parent molecule.

Figure 3 shows a typical photofragment TOF coincidence map, allowing clear identification of fragmentation events as specific final channels. Photodissociation into correlated $F + F^-$ products are marked by the dotted contour (a), with the neutral F arriving before the parent ion TOF, while the decelerated anionic fragment arrives at a clearly resolved time delay. Contour (b)

indicates the dissociative detachment channel with two correlated neutral products. Contour (c) indicates cation-neutral coincidence, while contour (d) marks the events corresponding to two correlated hits of F^+ products. The shaded area (e) corresponds to the parent F_2^- anions TOF, well separated from the product signals. The pair of dashed diagonal lines indicates the effective minimal 24ns time gap that is presently necessary for detection of two clearly separated hits. Contour (f) indicates the expected location of the $F^- + F^+$ ion-pair channel that is a significant ionization mechanism for neutral F_2.[36,45] However, the few events corresponding to $F^- + F^+$ shown here can be attributed to a random coincidence background based on systematic center of mass momentum analysis.

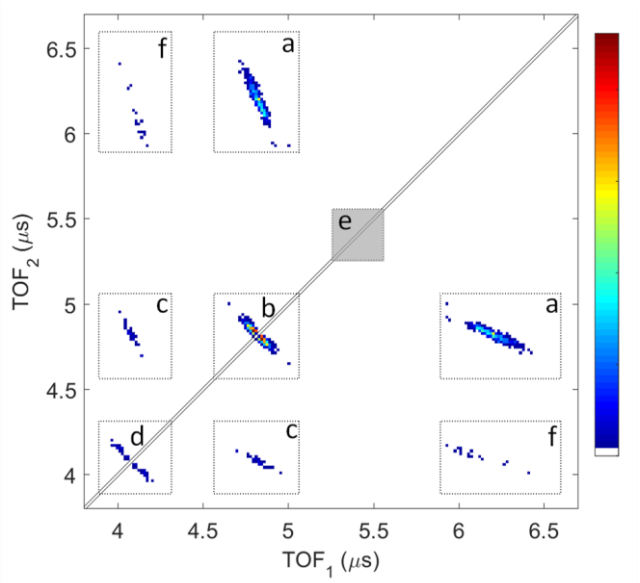

Figure 3: Photofragment TOF coincidence map. The map is symmetrized under exchange of fragment order. Contour (a) marks correlated F^- + F events, contour (b) marks F + F, (c) indicates double detachment F + F^+ events, and (d) marks F^+ + F^+ Coulomb explosion events. The shaded area (e) corresponds to the TOF of parent F_2^-. Contour (f) indicates the calculated TOF region for a possible F^- + F^+ ion pair channel.

RESULTS AND DISCUSSION:

Figure 4a shows the dependence of the different product yields on the laser peak intensity that is varied by changing "z", the displacement of the laser focal point from the F_2^- anion target. The peak laser intensity in the laser-ion interaction region corresponding to different z-scan steps reaches a maximum of ~10^{16} W/cm^2 at z = 0 and decreases with increasing z. Due to the decreasing interaction volume with increasing intensity, non-linear processes exhibit maximal yields at specific "z_{max}" positions.[37] The peak laser intensity at the z_{max} position can be directly

related, by a geometric factor of ~3, to the saturation intensity of each non-linear process.[37] One can clearly observe that the (F^- + F) channel yield as a function of z-scan position, shown by full dots in figure 4a, does not exhibit a peak, as expected for a saturated one photon process.[37] In contrast, the non-linear dissociative detachment (F + F), represented by full squares in figure 4a, exhibits maximal yield at z ~ 12 mm. The yield of rare multiple-detachment events are multiplied by 20 for comparison, empty circles representing the dissociative double-detachment (F + F^+) yield, for which maximum yield is measured at z ~ 6 mm. Multiple ionization leading to a Coulomb explosion (F^+ + F^+), which yields are represented by empty squares, appears for z < 10 mm. The observed trend is in accord with higher saturation intensities expected for the removal of each additional electron. By performing alternating measurements with the molecular F_2^- and atomic F^- samples, while maintaining the same laser conditions, we can directly compare the intensity dependence of atomic and molecular intense-field detachment mechanisms on a relative scale. Neutral F yields from an atomic F^- target, shown by the full squares in figure 4b, is saturated at peak intensities below $4 \cdot 10^{13}$ W/cm^2 at

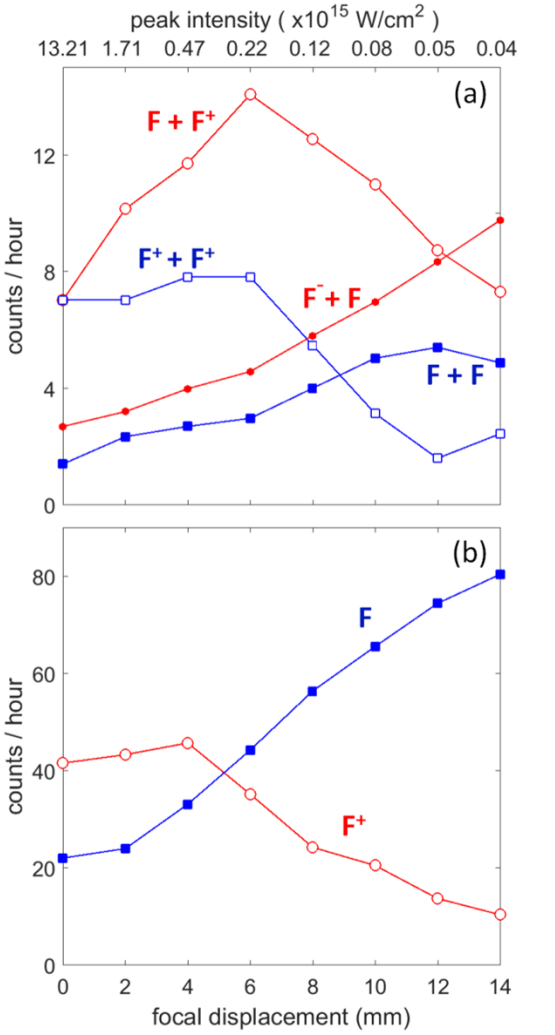

Figure 4: 'z-scan' analysis shows yield of events as a function of peak intensity, varied by displacing the focal point of the laser. Panel (a) shows coincidence product yields of intense-field interaction with F_2^-: (F^- + F) photodissociation, (F + F) dissociative detachment, (F + F^+) dissociative ionization yield x20, and (F^+ + F^+) Coulomb explosion yield x20. Panel (b) shows the simultaneously measured yields of intense-field interaction with atomic F^-: photodetachment yield of neutral F (x $^1/_{50}$) and double-detachment producing F^+.

focal displacements beyond 14mm. Double-detachment of the atomic F^- anion to produce F^+ is represented by empty circles and exhibits maximal yield at $z_{max} \sim 4$mm. As lower "z" positions that are closer to the laser focal point correspond to higher peak intensities, the observed z-scan dependencies are in agreement with previously reported enhancement of double- and multiple-detachment mechanisms in molecular compared with atomic systems.[19] In particular, one can compare the F^- double-detachment dependence on peak intensity presented in figure 4b to the triple-detachment of the molecule resulting in $F^+ + F^+$ in figure 4a, which displays a similar intensity dependence in spite of a significantly higher energy threshold. This in agreement with a similar trend reported for molecular SF_6^- and $F^-\cdot(NF_3)_n$ cluster anions.[19,21] Nevertheless, photodissociation is the predominant process in F_2^-, as can be expected from the favorable energetics that require only one 800 nm photon.

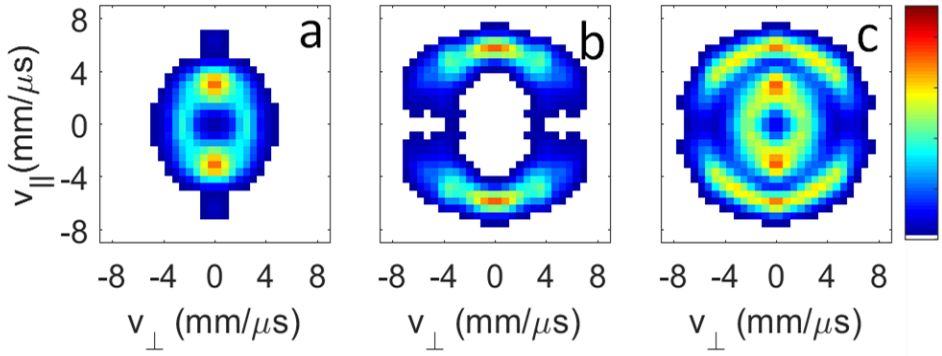

Figure 5: Dissociation velocity probability distribution for the F^- + F channel, in parallel and perpendicular to the laser polarization. (a) photodissociation with intense 800 nm pulses, (b) low intensity 400 nm and (c) with both 800 and 400 nm.

By disentangling the different final channels on an event-by-event basis, we measure the KER and angular distributions with respect to the laser polarization axis separately for each dissociative channel. Figure 5a shows the F^- + F photodissociation probability distribution $P(V_{||},V_\perp)$ of the velocity component parallel and perpendicular to the intense 800 nm linear laser polarization. High KER events with dissociation velocities of ~6 mm/μs, corresponding

energetically to two-photon absorption, can be observed to dissociate along the laser polarization. The majority of events contribute to a more isotropic distribution at low KER with velocities around 3 mm/μs. The spread of dissociation velocities as well as the non-trivial angular distribution indicate the contribution of non-linear photodissociation mechanisms also to low KER events. In comparison, Figure 5b shows the F^- + F velocity distribution recorded with low field 400 nm photodissociation. These higher velocity events correspond to dissociation on the $^2\Sigma_g^+$ leading asymptotically to the F^- ground state and a F* state, which is excited by a 50 meV spin-orbin splitting relative to the F ground state.[46] The alignment of the dissociation axis angle θ with respect to the laser polarization is characterized by an average $\langle\cos^2\theta\rangle = 0.6 \pm 0.03$, in agreement with the expected parallel transition and a $\cos^2\theta$ angular distribution.[47,48] Figure 5c shows the F + F^- velocity distribution recorded with both 400nm and 800nm pulses interacting with the molecular ions, demonstrating that the photodissociation on the $^2\Sigma_g^+$ and the $^2\Pi_u$ are clearly resolved both by their angular distribution and KER.

Figure 6a shows the 3D KER distribution for F^- + F dissociation corresponding to the velocity distribution is shown in Figure 5c. The two distinct low and high KER peaks correspond respectively to photodissociation by the intense 800 nm pulse, and photodissociation on the $^2\Sigma_g^+$ state, excited by 400 nm photons. The center of the high KER peak is fitted with a Gaussian shape centered at 1.79 eV shown by the full line (red color online). By energy conservation, the ground state dissociation energy D_0 is derived by subtracting the measured KER and the internal product energy from the 400 nm photon energy. Taking into account the 50 meV spin-orbit excitation of the $^2\Sigma_g^+$ dissociation F* product, we obtain $D_0 = 1.26 \pm 0.03$ eV.

Photodissociation on the $^2\Pi_g$ curve, following absorption of a single 800 nm photon can therefore be expected to result in a ~0.29 eV KER and a $\sin^2\theta$ angular distribution characteristic of a perpendicular transition, characterized by a $\langle\cos^2\theta\rangle = 0.2$. However, the observed KER peak is significantly broadened towards higher KER, above the combined width of the expected photon energy bandwidth and experimental resolution. Furthermore, careful examination of the velocity distribution presented in Figure 5a reveals a KER dependent angular distribution within the low velocity ring. The orientation of photodissociation events with KER $\leq$ 0.4 eV is characterized by an average $\langle\cos^2\theta\rangle = 0.32$. In contrast, blue shifted KER events, in the range of 0.65 < KER < 1.15 eV exhibit a $\langle\cos^2\theta\rangle = 0.54$. Thus, taking into account the finite experimental energy resolution, the observed velocity distribution can be consistent with a combination of the expected perpendicular transition and a higher KER contribution preferentially aligned parallel to the laser polarization, possibly due to the strong laser fields even at moderate focusing of the 800 nm pulse.

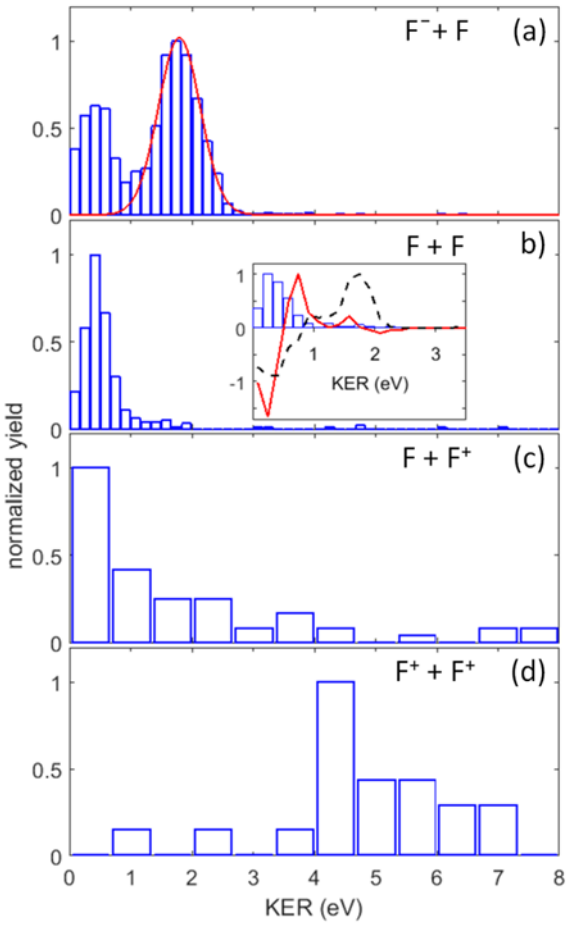

Figure 6: KER spectra of the (a) F^- + F photodissociation with both 800 nm and 400 nm pulses, with the full line (red online) representing the fitted $^2\Sigma_g^+$ dissociation component with KER centered around 1.79 eV. (b) F + F intense-field dissociative detachment, (c) F + F^+ dissociative ionization and (d) F^+ + F^+ Coulomb explosion channel. In the inset of panel (b): the bar plot shows the F + F KER spectrum with the intense 800 nm pulse arriving at negative time delays relative to the 400 nm pulse. The dashed dark line and the full line (red online) show the difference KER spectra measured for positive time delays and for time overlapping two colors respectively.

The KER spectrum corresponding to the F + F dissociative detachment channel is shown in Figure 6b. The low KER peak, associated with one 800nm photon dissociation energy, supports a sequential two-step mechanism of photodissociation at relatively low field intensities during the rising edge of the ultrafast pulse, followed by detachment of the atomic anion in the peak of the intense pulse. Due to the finite detection dead time between simultaneous hits, the exact angular distribution of the F + F is not presented. Nevertheless, a significant yield of two neutral fragments emitted perpendicular to the laser polarization is in agreement with the proposed sequential mechanism. Such a sequential mechanism can be confirmed by time resolved two color pump-probe experiments, taking advantage of the clearly resolved high KER peak corresponding to 400 nm photodissociation on the $^2\Sigma_g^+$ state. The inset of figure 6b shows the dissociative detachment KER spectrum dependence on the time delay of the intense 800 nm pulse with respect to the 400 nm pulse. At negative time delays, the KER spectrum represented by empty bars is essentially identical to the 800 nm only spectrum as the weaker 400 nm pulse alone does not produce pairs of correlated neutral products. The dashed and full lines show the difference KER spectra that are obtained by subtracting the negative time KER spectrum from the spectra measured respectively with positive time delay and with time overlapping pump-probe pulses. The difference KER spectrum of overlapping 800nm and 400nm pulses exhibits an enhancement of the blue shifted edge of the low KER peak. At positive time delays a new high KER peak appears at the expense of the low KER

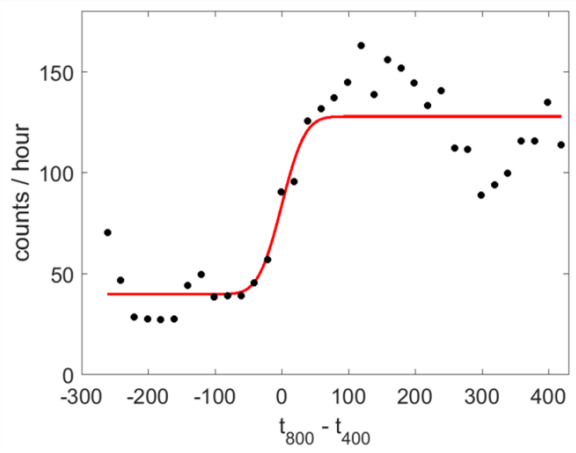

Figure 7: Time resolved rise of the high KER peak in the F + F coincidence channel, corresponding to photodissociation by a 400 nm photon on the $^2\Sigma_g^+$ state followed by detachment of the F^- product by a time delayed intense 800nm pulse. The fluctuations around the fitted curve are within the statistical errorbars.

events. The emerging high KER peak is in agreement with the proposed sequential mechanism of photodissociation on the $^2\Sigma_g^+$ state releasing ~1.79 eV and a subsequent detachment of the F^- product by the intense 800 nm pulse. Figure 7 shows the time resolved onset of the high KER peak that is limited by the cross correlation of the ~35 fs pump and probe pulses, in agreement with a prompt dissociation on the $^2\Sigma_g^+$ curve. Thus, photodissociation can be completed within the duration of the intense 35 fs pulse, facilitating a sequential mechanism of early photodissociation followed by detachment of the atomic anion.

The removal of a second electron from the system leads to dissociation forming $F + F^+$ coincidence. No stable F_2^+ product was observed within the experimental sensitivity, which is limited by a finite background of single hit events. Figure 6c shows the KER spectrum of the dissociative ionization $F + F^+$ channel. Similar to the case of dissociative detachment, the spectrum is dominated by a low KER peak that can be assigned to a mechanism of photo-dissociation followed by double-detachment of the atomic F^- product within the same laser pulse. However, a significant contribution of non-sequential double-detachment of undissociated F_2^- is indicated by the presence of relatively high KER events in the range between 2 to 5 eV. Figure 8 shows the partial yields of low and high KER components as a function of laser peak intensity, showing how at peak intensities above $2 \cdot 10^{14}$ W/cm^2 a non-sequential double-detachment, distinguished by high KER, competes with the step-wise

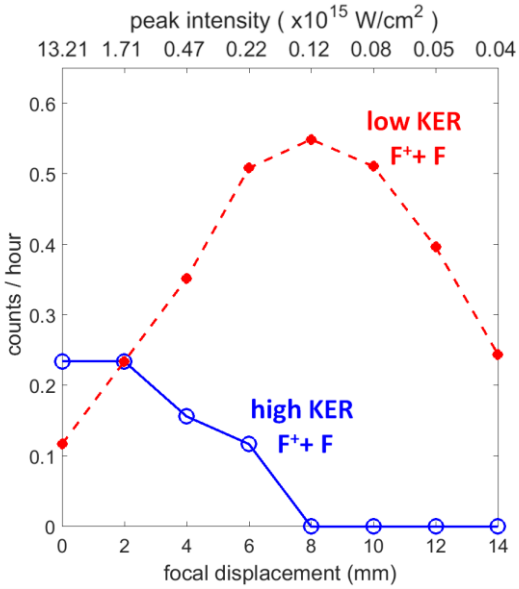

Figure 8: Partial yields of the low KER (full dots) and high KER (empty circles) dissociative ionization ($F + F^+$) events as a function of laser peak intensity, varied by displacement from the focal point.

mechanism contributing to low KER only. A similar high KER tail in dissociative ionization was also reported for intense-field double-detachment of the SF_6^- molecular anion.[20] Kandhasamy *et al*. proposed that the high KER tail results from frustrated ionization,[20] producing highly repulsive Rydberg states. The dication core of such a state results in high KER similar to a Coulomb explosion, albeit with only one ionic product.[49] The dashed line in Figure 1c illustrates a repulsive curve of a F_2^+ Rydberg state, one of an infinite number of such states that converge to the dication limit. Although multiple detachment of SF_6^- was shown to produce correlated cation products, it was found to be accompanied by complete disintegration of the molecule that prevented reliable analysis of Coulomb explosion events. Figure 6d shows the KER spectrum of correlated $F^+ + F^+$ products of intense-field interaction with the diatomic F_2^-. As opposed to all other channels, $F^+ + F^+$ KER spectrum excludes contribution of a sequential mechanism that would be branded by the low KER in the photodissociation stage. On one hand, a purely Coulombic explosion of two charges initiated from the 1.88 Å equilibrium F_2^- bond length can release 7.66 eV. On the other hand, considering the remaining valence electrons of the F_2^{2+} dication one can expect screening of the pure Coulomb repulsion and a correspondingly lower KER. Lower KER could also stem from bond elongation during the interaction with the intense laser pulse.[50] The high KER in the 4-8 eV range is therefore in agreement with a non-sequential mechanism that involves multiple detachment of the F_2^- and a dissociation on a highly repulsive Coulomb potential as illustrated in Figure 1c.

CONCLUSIONS:

Four competing processes are observed in intense fs laser pulse interaction with the molecular F_2^- anion. F^- + F photodissociation channel shows a combination of a linear transition to the $^2\Pi_g$ state, occurring preferentially for F_2^- molecules aligned perpendicularly to the 800 nm laser polarization, as well as a non-linear contribution leading to a higher KER parallel to the laser polarization. With increasing laser peak intensity, F + F products of detachment exhibit a similar KER structure assigned to photodetachment of atomic anions produced by early photodissociation within the same pulse. A sequential mechanism is supported also by two color pump-probe measurements that allow clear identification of prompt dissociation on the $^2\Sigma_g^+$ curve by the low field 400 nm pulse, followed by detachment of the atomic anion intermediate. The KER measured for low field photodissociation with 400 nm photons allows direct experimental determination of the F_2^- ground state dissociation energy D_0=1.26±0.03 eV, in rough agreement with the ~1.31 eV estimates based on indirect measurements,[24] and within the errorbars of the 1.21±0.07 eV threshold energy of collision induced dissociation.[51] The calculated ab-initio values found in the literature for the ground state dissociation energy are in the 1.19eV -1.4eV range,[31–33,35] also in rough agreement with the direct experimental measurement presented here. At peak intensities on the order of 10^{14} W/cm^2, ionization producing F + F^+ exhibits competition between sequential and non-sequential mechanisms reflected in the measured KER spectra as a function of peak intensity. At comparable peak intensities above 10^{14} W/cm^2, Coulomb explosion events with characteristically high KER in the 4-8 eV range exhibit a strictly non-sequential nature. The missing sequential contribution in spite of saturated photodissociation supports a significant enhancement of multiple detachment of the undissociated molecular anion system compared with ionization of the atomic neutral F products

of photodissociation. Moreover, the range of high KER observed in the $F + F^+$ channel, extending to the KER observed in Coulomb explosion events is in agreement with a mechanism involving highly repulsive Rydberg states with a dication core proposed by Kandhasamy *et al*.[20] Further theoretical work is needed to explain the efficient non-sequential multiple-detachment mechanism, which is now experimentally characterized for the relatively simple diatomic F_2^- anion.

References

(1) Kiyan, I. Y.; Helm, H. Production of Energetic Electrons in the Process of Photodetachment of F^-. *Phys. Rev. Lett.* **2003**, 90, 183001.

(2) Pedregosa-Gutierrez, J.; Orr, P. A.; Greenwood, J. B.; Murphy, A.; Costello, J. T.; Zrost, K.; Ergler, T.; Moshammer, R.; Ullrich, J. Evidence for Rescattering in Intense, Femtosecond Laser Interactions with a Negative Ion. *Phys. Rev. Lett.* **2004**, 93, 223001.

(3) Gazibegović-Busuladžić, a.; Milošević, D. B.; Becker, W. High-Energy above-Threshold Detachment from Negative Ions. *Phys. Rev. A* **2004**, 70, 53403.

(4) Hassouneh, O.; Law, S.; Shearer, S. F. C.; Brown, a. C.; van der Hart, H. W. Electron Rescattering in Strong-Field Photodetachment of F^-. *Phys. Rev. A* **2015**, 91, 31404.

(5) Albeck, Y.; Kandhasamy, D. M.; Strasser, D. Multiple Detachment of the SF_6^- Molecular Anion with Shaped Intense Laser Pulses. *J. Phys. Chem. A* **2014**, 118, 388–395.

(6) Corkum, P. Plasma Perspective on Strong Field Multiphoton Ionization. *Phys. Rev. Lett.* **1993**, 71, 1994–1997.

(7) Larochelle, S.; Talebpour, A.; Chin, S. L. Non-Sequential Multiple Ionization of Rare Gas Atoms in a Ti:Sapphire Laser Field. *J. Phys. B At. Mol. Opt. Phys.* **1998**, 31, 1201–1214.

(8) Feuerstein, B.; Moshammer, R.; Fischer, D.; Dorn, A.; Schröter, C. D.; Deipenwisch, J.; Crespo Lopez-Urrutia, J. R.; Höhr, C.; Neumayer, P.; Ullrich, J.; et al. Separation of Recollision Mechanisms in Nonsequential Strong Field Double Ionization of Ar: The Role of Excitation Tunneling. *Phys. Rev. Lett.* **2001**, 87, 43003.

(9) Rudenko, A.; Zrost, K.; Feuerstein, B.; de Jesus, V. L. B.; Schröter, C. D.; Moshammer, R.; Ullrich, J. Correlated Multielectron Dynamics in Ultrafast Laser Pulse Interactions with Atoms. *Phys. Rev. Lett.* **2004**, 93, 253001.

(10) Posthumus, J. The Dynamics of Small Molecules in Intense Laser Fields. *Reports Prog. Phys.* **2004**, 67, 623–665.

(11) Sheehy, B. 10 Chemical Processes in Intense Optical Fields. *Annu. Reports Sect. "C" (Physical Chem.* **2001**, 97, 383–410.

(12) Sheehy, B.; DiMauro, L. F. Atomic and Molecular Dynamics in Intense Optical Fields. *Annu. Rev. Phys. Chem.* **1996**, 47, 463–494.

(13) Dörner, R.; Weber, T.; Weckenbrock, M.; Staudte, A.; Hattass, M.; Schmidt-Böcking, H.; Moshammer, R.; Ullrich, J. Multiple Ionization in Strong Laser Fields. In *Advances In Atomic, Molecular, and Optical Physics*; 2002; Vol. 48, 1–34.

(14) Gazibegović-Busuladžić, A.; Milošević, D. B.; Becker, W.; Bergues, B.; Hultgren, H.; Kiyan, I. Y. Electron Rescattering in Above-Threshold Photodetachment of Negative Ions. *Phys. Rev. Lett.* **2010**, 104, 103004.

(15) Ostrovsky, V. N. Multiphoton Detachment with Atom Excitation: Explicit Three-Step Quantum Theory. *J. Phys. B At. Mol. Opt. Phys.* **2003**, 36, 2647–2656.

(16) Frolov, M. V.; Manakov, N. L.; Pronin, E. A.; Starace, A. F. Model-Independent Quantum Approach for Intense Laser Detachment of a Weakly Bound Electron. *Phys. Rev. Lett.* **2003**, 91, 53003.

(17) Kamta, G. L.; Starace, A. F. Elucidating the Mechanisms of Double Ionization Using Intense Half-Cycle, Single-Cycle, and Double Half-Cycle Pulses. *Phys. Rev. A* **2003**, 68, 43413.

(18) Bergues, B.; Kiyan, I. Y. Two-Electron Photodetachment of Negative Ions in a Strong Laser Field. *Phys. Rev. Lett.* **2008**, 100, 143004.

(19) Albeck, Y.; Lerner, G.; Kandhasamy, D. M.; Chandrasekaran, V.; Strasser, D. Intense Field Double Detachment of Atomic versus Molecular Anions. *Phys. Rev. A* **2015**, 92, 61401.

(20) Kandhasamy, D. M.; Albeck, Y.; Jagtap, K.; Strasser, D. 3D Coincidence Imaging Disentangles Intense Field Double Detachment of SF_6^-. *J. Phys. Chem. A* **2015**, 119, 8076–8082.

(21) Albeck, Y.; Lerner, G.; Kandhasamy, D. M.; Chandrasekaran, V.; Strasser, D. Intense-Field Double Detachment of Electrostatically Bound $F^-(NF_3)_n$ Cluster Anions. *J. Phys. Chem. A* **2016**, 120, 3246–3252.

(22) Alexander, M. L.; Levinger, N. E.; Johnson, M. A.; Ray, D.; Lineberger, W. C. Recombination of Br_2^- Photodissociated within Mass Selected Ionic Clusters. *J. Chem. Phys.* **1988**, 88, 6200–6210.

(23) Papanikolas, J. M.; Gord, J. R.; Levinger, N. E.; Ray, D.; Vorsa, V.; Lineberger, W. C. Photodissociation and Geminate Recombination Dynamics of Iodine (I_2^-) in Mass-Selected Iodine-Carbon Dioxide (I_2^- (CO2)n) Cluster Ions. *J. Phys. Chem.* **1991**, 95, 8028–8040.

(24) Dojahn, J. G.; Chen, E. C. M.; Wentworth, W. E. Characterization of Homonuclear Diatomic Ions by

Semiempirical Morse Potential Energy Curves. 1. The Halogen Anions. *J. Phys. Chem.* **1996**, 100, 9649–9657.
(25) Braïda, B.; Hiberty, P. C. Diatomic Halogen Anions and Related Three-Electron-Bonded Anion Radicals: Very Contrasted Performances of Møller−Plesset Methods in Symmetric vs Dissymmetric Cases. *J. Phys. Chem. A* **2000**, 104, 4618–4628.
(26) Chupka, W. A. Electron Affinities of Halogen Diatomic Molecules as Determined by Endoergic Charge Transfer. *J. Chem. Phys.* **1971**, 55, 2724–2733.
(27) Hultgren, H.; Kiyan, I. Y. Photodetachment Dynamics of F_2^- in a Strong Laser Field. *Phys. Rev. A* **2011**, 84, 15401.
(28) Walhout, P. K.; Alfano, J. C.; Thakur, K. A. M.; Barbara, P. F. Ultrafast Experiments on the Photodissociation, Recombination, and Vibrational Relaxation of I_2^-: Role of Solvent-Induced Solute Charge Flow. *J. Phys. Chem.* **1995**, 99, 7568–7580.
(29) Jefferys Greenblatt, B.; Zanni, M. T.; Neumark, D. M. Photodissociation Dynamics of the I_2^- Anion Using Femtosecond Photoelectron Spectroscopy. *Chem. Phys. Lett.* **1996**, 258, 523–529.
(30) Hoops, A. A.; Gascooke, J. R.; Faulhaber, A. E.; Kautzman, K. E.; Neumark, D. M. Fast Beam Studies of I_2^- and I_2^-·Ar Photodissociation. *Chem. Phys. Lett.* **2003**, 374, 235–242.
(31) Honigmann, M.; Buenker, R. J.; Liebermann, H.-P. Complex Configuration Interaction Calculations of the Cross Section for the Dissociative Electron Attachment Process $e^- + F_2 \rightarrow F_2^- \rightarrow F + F^-$ Using the Complex Basis Function Method. *J. Comput. Chem.* **2012**, 33, 355–362.
(32) Hazi, A. U.; Orel, A. E.; Rescigno, T. N. Ab Initio Study of Dissociative Attachment of Low-Energy Electrons to F_2. *Phys. Rev. Lett.* **1981**, 46, 918–922.
(33) Ingr, M.; Meyer, H.-D.; Cederbaum, L. S. Potential Energy Curve of the X 2 Sigma U + Resonance State of F 2 - Computed by CAP/CI. *J. Phys. B At. Mol. Opt. Phys.* **1999**, 32, L547–L556.
(34) Brems, V.; Beyer, T.; Nestmann, B. M.; Meyer, H.-D.; Cederbaum, L. S. Ab Initio Study of the Resonant Electron Attachment to the F_2 Molecule. *J. Chem. Phys.* **2002**, 117, 10635–10647.
(35) Rescigno, T. N.; Bender, C. F. The Stability of the F_2^- Ion: A Model for Dissociative Attachment. *J. Phys. B At. Mol. Phys.* **1976**, 9, L329–L332.
(36) Berkowitz, J.; Chupaka, W. A.; Guyon, P. M.; Holloway, J. H.; Spohr, R. Photoionization Mass Spectrometric Study of F_2, HF, and DF. *J. Chem. Phys.* **1971**, 54, 5165–5180.
(37) Albeck, Y.; Kandhasamy, D. M.; Strasser, D. Z-Scan Method for Nonlinear Saturation Intensity Determination, Using Focused Intense Laser Beams. *Phys. Rev. A* **2014**, 90, 53422.
(38) Harland, P. W.; Franklin, J. L. Partitioning of Excess Energy in Dissociative Resonance Capture Processes. *J. Chem. Phys.* **1974**, 61, 1621–1636.
(39) Ruckhaberle, N.; Lehmann, L.; Matejcik, S.; Illenberger, E.; Bouteiller, Y.; Periquet, V.; Museur, L.; Desfrançois, C.; Schermann, J.-P. Free Electron Attachment and Rydberg Electron Transfer to NF_3 Molecules and Clusters. *J. Phys. Chem. A* **1997**, 101, 9942–9947.
(40) Wiley, W. C.; McLaren, I. H. Time-of-Flight Mass Spectrometer with Improved Resolution. *Rev. Sci. Instrum.* **1955**, 26, 1150–1157.
(41) Spectra-Physics; Newport Co. Solstice Ace ®.
(42) Urbain, X.; Bech, D.; Van Roy, J.-P.; Géléoc, M.; Weber, S. J.; Huetz, A.; Picard, Y. J. A Zero Dead-Time Multi-Particle Time and Position Sensitive Detector Based on Correlation between Brightness and Amplitude. *Rev. Sci. Instrum.* **2015**, 86, 23305.
(43) Lee, S. K.; Cudry, F.; Lin, Y. F.; Lingenfelter, S.; Winney, A. H.; Fan, L.; Li, W. Coincidence Ion Imaging with a Fast Frame Camera. *Rev. Sci. Instrum.* **2014**, 85, 123303.
(44) SIMION: Ion Optics Software, SIS, Inc.
(45) DeCorpo, J. J.; Steiger, R. P.; Franklin, J. L.; Margrave, J. L. Dissociation Energy of F_2. *J. Chem. Phys.* **1970**, 53, 936–938.
(46) Kramida, A., Ralchenko, Yu., Reader, J., and N. A. T. NIST Atomic Spectra Database (ver. 5.3), [2016, November 20]. National Institute of Standards and Technology, Gaithersburg, MD.
(47) Zare, R. N.; Herschbach, D. R. Doppler Line Shape of Atomic Fluorescence Excited by Molecular Photodissociation. *Proc. IEEE* **1963**, 51, 173–182.
(48) Zare, R. N. Photoejection Dynamics. *Molecular Photochemistry*. 1972, 1–37.
(49) McKenna, J.; Sayler, A. M.; Gaire, B.; Kling, N. G.; Esry, B. D.; Carnes, K. D.; Ben-Itzhak, I. Frustrated Tunnelling Ionization during Strong-Field Fragmentation of D_3^+. *New J. Phys.* **2012**, 14, 103029.
(50) Légaré, F.; Litvinyuk, I. V; Dooley, P. W.; Quéré, F.; Bandrauk, A. D.; Villeneuve, D. M.; Corkum, P. B. Time-Resolved Double Ionization with Few Cycle Laser Pulses. *Phys. Rev. Lett.* **2003**, 91, 93002.

(51) Wenthold, P. G.; Squires, R. R. Bond Dissociation Energies of F_2^- and HF_2^-. A Gas-Phase Experimental and G2 Theoretical Study. *J. Phys. Chem.* **1995**, 99, 2002–2005.

ACKNOWLEDGMENT

The authors gratefully acknowledge financial assistance from the European Research Council through grant number 306783 as well as from the US-Israel Bi-national Science Foundation grant number 2014071.